

**Distribution Agreement**

In presenting this thesis as a partial fulfillment of the requirements for a degree from Emory University, I hereby grant to Emory University and its agents the non-exclusive license to archive, make accessible, and display my thesis in whole or in part in all forms of media, now or hereafter now, including display on the World Wide Web. I understand that I may select some access restrictions as part of the online submission of this thesis. I retain all ownership rights to the copyright of the thesis. I also retain the right to use in future works (such as articles or books) all or part of this thesis.

Ria Gupta

April 12, 2022

GDF15 Produced by the Failing Heart is Associated with Cardiac Cachexia

by

Ria Gupta

Dr. Michael Burke  
Adviser

Emory College of Arts and Sciences

Dr. Michael Burke  
Adviser

Dr. Steven L'Hernault  
Committee Member

Dr. Roger Deal  
Committee Member  
2022

GDF15 Produced by the Failing Heart is Associated with Cardiac Cachexia

by

Ria Gupta

Dr. Michael Burke  
Adviser

An abstract of  
a thesis submitted to the Faculty of Emory College of Arts and Sciences  
of Emory University in partial fulfillment  
of the requirements of the degree of  
Bachelor of Science with Honors

Emory College of Arts and Sciences

2022

Abstract  
GDF15 Produced by the Failing Heart is Associated with Cardiac Cachexia  
By Ria Gupta

Heart failure (HF) is a disease that affects 6.2 million adults in the United States with a 5-year mortality rate of 52.6%. One complication of HF is cachexia. Cachexia is the involuntary non-edematous weight loss that cannot be reversed solely by nutritional intake. Marked by continuous fat and muscle breakdown via metabolic imbalances, cachexia presents with anorexia and hypophagia. This chronic metabolic alteration is correlated with a specific increase of growth differentiation factor 15 (GDF15), suggesting this molecule as a driver of cachexia. GDF15 is a stress induced cytokine that increases in chronic diseases and continued nutritional and metabolic bodily stress. Although cachexia and elevated GDF15 levels are present in HF, no biological effect has been established between GDF15 in cardiac pathophysiology. Our hypothesis is that GDF15 is a myocardial derived hormone that causes anorexia and cardiac cachexia. My results suggest that GDF15 is a driver of cachexia through decreased fat and muscle mass, food intake, and altered body parameters. Our lab used a GDF15 KO mouse model that incurs HF through a mutation in the phospholamban (PLN) gene. This mutation alters calcium signaling in cardiomyocytes, a hallmark feature of HF in humans. I have used mouse models and lab techniques including Q-PCR, ELISA and RNA sequencing (RNA-seq), to study the role of GDF15 in HF. We establish that GDF15 is increased in a mouse model of HF, is secreted specifically by the failing heart, and alters peripheral metabolic changes in the body. While further experimentation is needed to test a direct role of GDF15 in cachexia, these and future findings may lead to novel drug therapeutics to treat HF and cachexia.

GDF15 Produced by the Failing Heart is Associated with Cardiac Cachexia

by

Ria Gupta

Dr. Michael Burke  
Adviser

A thesis submitted to the Faculty of Emory College of Arts and Sciences  
of Emory University in partial fulfillment  
of the requirements of the degree of  
Bachelor of Science with Honors  
Emory College of Arts and Sciences

2022

## Acknowledgements

Dr. Michael Burke  
Andrew Antolic  
Da Young Lee  
Talha Ijaz  
Zhe Jiao

Table of Contents

Introduction .....5

*Heart Function and Failure.....5*

*Cardiac Cachexia.....9*

*Cachexia and Growth Differentiation Factor 15 .....11*

*PLN<sup>R9C</sup> Mice Models .....15*

Methods ..... 18

Results ..... 23

Specific Aims..... 28

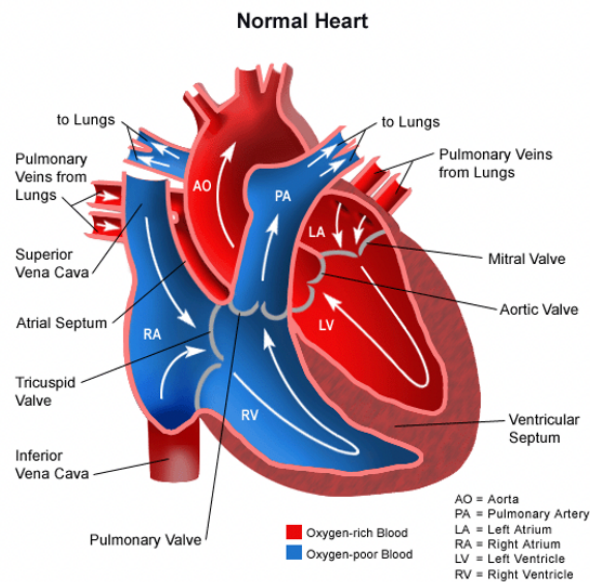
Discussion..... 32

References..... 37

## INTRODUCTION

### Heart Function and Failure

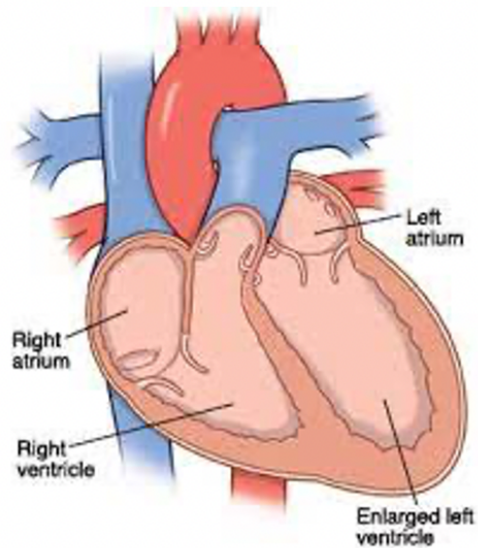
The heart is an essential organ that circulates blood to all other organs and tissues in the body. The human heart has 4 chambers: 2 atria receive blood and transmit it to the 2 ventricles, which pump blood out of the heart to the body (Figure 1). The right ventricle pumps blood to the lungs where it is oxygenated while the left ventricle (LV) pumps this oxygenated blood throughout the rest of the body. Due to this central physiological function, damage to the heart is often life threatening. Indeed, cardiovascular disease is the commonest cause of death in the United States and worldwide.



<https://www.stanfordchildrens.org/en/topic/default?id=blood-circulation-in-the-fetus-and-newborn-90-P02362>

**Figure 1. Heart Anatomy.** Blood returns to the heart from the body via the inferior and superior vena cavae, which drain into the right atrium. Blood then flows from the right atrium to the right ventricle, which pumps it into the lungs where it is oxygenated during respiration. Blood from the lungs returns to the left atrium of the heart which passes blood into the left ventricle. The left ventricle then circulates blood to all organs and tissues in the body.

Heart disease can manifest as an acute insult such as a myocardial infarction (MI, commonly called a “heart attack”) or can present as a chronic progressive disorder such as heart failure (HF). HF is a complex syndrome whereby the ability of the ventricles to circulate blood through the body becomes impaired (Figure 2). This leads to a reduced ability to exercise or perform daily activities and produces symptoms of shortness of breath (termed dyspnea by physicians), fatigue, and bodily edema that substantially reduces the quality of life for these individuals (Figure 3).



<https://fairviewmnhs.org/patient-education/115853EN>

**Figure 2. Dilated left ventricle causes HF.** The left ventricle is the main pumping chamber of the human body. When this ventricle is dilated, it alters normal cardiac function such as cardiac contractility. It also leads to severe cardiovascular events and HF.



[https://www.physio-pedia.com/index.php?title=Congestive\\_Heart\\_Failure\\_-\\_Pharmacotherapy&lang=en](https://www.physio-pedia.com/index.php?title=Congestive_Heart_Failure_-_Pharmacotherapy&lang=en)

**Figure 3. Patient with Heart Failure.** Common functional limitations in heart failure include dyspnea due to excessive pulmonary edema from left ventricular failure.

HF is frequently a secondary consequence of a wide range of cardiac and systemic conditions that damage the ventricles, most commonly ischemic heart disease<sup>1</sup> (Table 1). However, HF can also be a primary disorder of the heart caused by a specific set of genetic mutations or without a clear antecedent cause.

Table 1. Causes of Heart Failure	
Ischemic Heart Disease	Endocrine Disorders
Genetic Mutations	Infiltration in Cardiac tissue
Hypertension	Peripartum
Coronary Heart Disease	Congenital Heart Disease
Persistent Tachycardia	Cardiac Infections
Valvular Heart Disease	Diabetes
Myocarditis	Cardiotoxic Drugs

Kemp et. al. Cardiovasc Pathol. 2012  
 Pazos-Lopez et. al. Vasc Health Risk Manag. 2011

HF is a leading cause of morbidity. The prevalence of HF in the United States is 6.2 million adults; the average 40-year old has a 1 in 5 chance of developing HF during their lifetime<sup>2</sup>. In spite of a bevy of effective therapies, HF accounts for more than 1 million hospitalizations each year in the United States and causes a staggering \$30.7 billion per year in annual costs, a number expected to more than double by the year 2030. Finally, mortality in HF is very high. After a diagnosis of HF, mortality is 10% at 30 days, 22% at 1 year, and 52% at 5 years<sup>2, 3</sup>. Of the 9 commonest forms of cancer, which collectively account for ~92% of all cancers in the United States, only lung cancer (78.3%) has a 5-year mortality that is close to or exceeds that of HF (Table 2).

<b>Table 2. Disease</b>	<b>Prevalence</b>	<b>5 Year Mortality Rate</b>
Heart Failure	6.2 million	52.6%
Cancer*	15.8 million	32.3%
Breast cancer	3.67 million	9.7%
Prostate cancer	3.24 million	2.5%
Colon and Rectum cancer	1.36 million	35.3%
Melanoma	1.29 million	6.7%
Thyroid cancer	893,094	1.7%
Uterine cancer	813,861	18.9%
Bladder cancer	723,745	31.9%
<i>Lung cancer</i>	<i>582,631</i>	<i>78.3%</i>
Renal cancer	582,727	24.4%

**\*All forms of solid organ and blood-stream cancer excepting basal and squamous cell skin cancers, which are not tracked and are virtually never fatal.**

<http://seer.cancer.gov/statfacts/>

HF is a systemic disease. As the heart begins to fail, a number of compensatory mechanisms attempt to restore normal cardiac output to the rest of the body. These include

activation of the sympathetic nervous system and the renin-angiotensin-aldosterone system<sup>4</sup>. The increase in sympathetic output increases heart rate and contractility, while activation of the renin-angiotensin-aldosterone system enhance fluid and sodium retention, increasing blood volume. Collectively, these physiologic changes produce an increase in cardiac output to the body. However, with chronic activation these compensatory mechanisms actually become a driver of HF progression by triggering vascular changes that increase cardiac work and causing fluid overload, both of which lead to the hallmark symptoms of HF<sup>5</sup>. Left unchecked, cardiac output eventually falls below levels necessary to meet basal metabolic demands (a pathophysiologic state called shock); the individual becomes symptomatic at rest and develops other organ dysfunction, a condition that is uniformly fatal without extreme interventions such as continuous intravenous medications, surgically implanted mechanical heart pumps or heart transplantation.

### Cardiac Cachexia

The systemic consequences of HF are myriad and include kidney and liver dysfunction, changes to the immune system, alterations in the vasculature, and a shift in metabolism. Some individuals also develop a condition called cachexia (termed cardiac cachexia when due to HF), which is unintentional weight loss that does not include the loss of edema fluid that has built up as a consequence of HF<sup>6</sup>. Cachexia is insidious in onset and can be difficult to detect, especially in those who are or were obese. However, cachexia is quite common and is found in ~20% of HF patients (with some studies suggesting rates as high as 40%<sup>7</sup>). Cachexia becomes more prevalent as HF progresses. It might be present in up to 60% of patients who are awaiting heart transplantation<sup>8</sup>, and it is an independent predictor of death in those who receive a heart transplant<sup>9, 10</sup>. Importantly, cardiac cachexia has an exceedingly high mortality rate, with 50% being dead within 18 months of diagnosis with cachexia<sup>11</sup>. Despite this serious outcome, little is

known about the molecular mechanisms that cause cachexia in HF. **The overarching goal of our study is to characterize a putative driver of cardiac cachexia.**

Many theories exist as to the origin of cachexia in HF. In general, these hold that the neurohumoral imbalance and systemic inflammatory state that develops in HF leads to changes in appetite and altered metabolism, particularly in fat tissue and skeletal muscle. Neurohumoral contributions include imbalanced hormone levels in the renin-angiotensin system and vasopressin and alterations in the sympathetic nervous system. Systemic inflammation increases the circulation of inflammatory cytokines and macrophages. These alterations trigger an imbalance between catabolism and anabolism that results in progressive protein and fat degradation, and ultimately cachexia (Figure 4). However, the evidence to support this interpretation is limited and indirect, and no cardiac derived mechanisms are known to cause cachexia in HF.

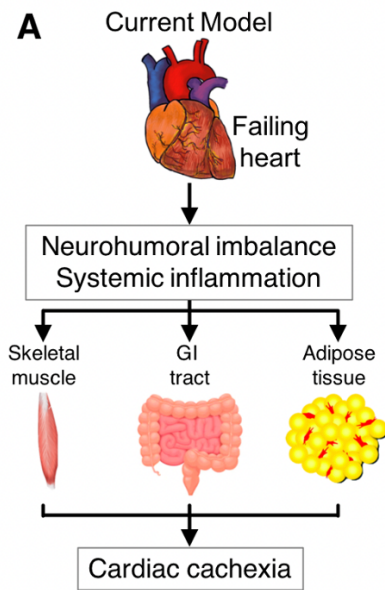


**Figure 4 . Possible mechanisms of cardiac cachexia in HF.** HF leads to activation of neurohormonal and inflammatory signaling networks. It is posited that these systemic processes indirectly influence other organs, leading to the cachectic state, but the direct signaling mechanisms involved remain unknown.

### Cachexia and Growth Differentiation Factor 15

Beyond HF, cachexia is a common manifestation of advanced stages of many chronic diseases including cancer, chronic kidney disease, chronic obstructive pulmonary disease, AIDS, tuberculosis and chronic inflammatory diseases such as rheumatoid arthritis. In cancer, it has long been hypothesized that tumor cell derived molecules alter the control of body weight, though the mechanisms were unclear. Recently, growth differentiation factor 15 (GDF15; previously known as macrophage inhibitory cytokine-1) has been identified as a tumor derived factor that causes cachexia<sup>12</sup>. GDF15 is produced by a number of cancers, and serum levels are higher in those with more advanced disease.

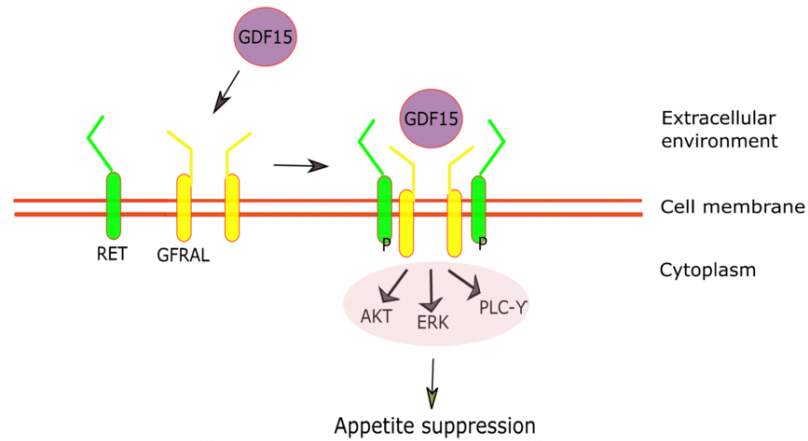
GDF15 is a stress-induced cytokine and a member of the transforming growth factor (TGF)- $\beta$  superfamily. It is upregulated in many disease states, yet its biologic function remained

unknown until very recently. In a landmark study, injection of recombinant GDF15 induced anorexia and weight loss in normal mice, an effect that was blocked by concomitant treatment with a GDF15 neutralizing antibody<sup>12</sup>. These authors also found that tumors that produce GDF15 are associated with weight loss in mice as compared to tumors that do not express GDF15. In transgenic mice, GDF15 overexpression caused anorexia and reduced fat and lean tissue mass, while GDF15 knockout (KO) mice have higher adiposity relative to wild type mice<sup>12-15</sup>.

Interestingly and unlike other entero-endocrine hormones (e.g., leptin), GDF15 does not respond to short term changes in caloric intake. Instead, GDF15 levels rise in the presence of chronic nutritional stress or after toxin ingestion. In these settings, GDF15 triggers an aversive response that changes feeding behavior<sup>15</sup>. Toxin exposure provides a straightforward example: GDF15 is produced in response to chemotherapy whereby it causes emesis and anorexia, as is commonly observed in humans receiving treatment for cancer<sup>16</sup>. Teleologically, the role of this aversive response may be to force a change in feeding or foraging behaviors in the animal when nutritional needs are not being met. However, this clearly results in a maladaptive response in the setting of a chronic illness such as HF.

In conjunction with its role in feeding, GDF15 levels were shown to correlate with activation of a specific set of neurons located in the area postrema of the brainstem, which happens to be the appetite center of the brain. Recent work has revealed that GDF15 binds to glial cell-derived neurotrophic factor (GDNF) receptor  $\alpha$ -like (GFRAL)<sup>17-20</sup>. This previously orphan receptor is only expressed in this region of the hindbrain and is not known to be expressed anywhere else in the body. Upon binding of GDF15 to GFRAL on the cell surface, GFRAL activates the receptor tyrosine kinase, Ret, which triggers downstream signaling via the AKT, ERK and phospholipase C pathways. The resultant neuronal activation triggers the

activation of nearby sympathetic neurons in the parabrachial nucleus, which then signals to the periphery via the sympathetic nervous system (Figure 5, 6). This signaling ultimately suppresses food intake and regulates body weight and can trigger metabolic alterations in peripheral tissues leading to catabolism.



Assadi et. al. 2020.

**Figure 5. GDF15 Interaction with GFRAL.** GDF15 binds to GFRAL on the cell surface. This triggers dimerization with RET, therefore causing RET activation. This activation allows for a signaling cascade where several signaling molecules such as AKT and ERK are phosphorylated for interaction.

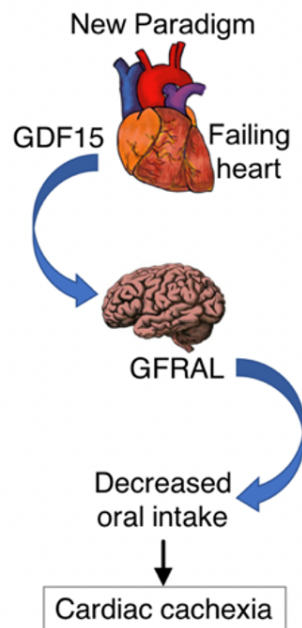


**Figure 6. Our overarching hypothesis to characterize a GDF15 mechanism of action.** We aim to establish that GDF15 is a cardiac specific hormone that interacts with GFRAL to induce cardiac cachexia.

GDF15 is a sensitive biomarker in both healthy populations and populations with cardiovascular disease<sup>21-26</sup> (Figure 7). Elevated levels of GDF15 portend a higher risk of cardiovascular events such as MI, HF, and stroke in healthy individuals. This holds true in patients with dilated cardiomyopathy (DCM), stable coronary artery disease, acute coronary syndromes, congenital heart disease, atrial fibrillation, and other chronic non-cardiac diseases<sup>21, 27-45</sup>. In patients with HF, higher levels of GDF15 correlate with a greater burden of symptoms, lower ejection fraction, and lower cardiac output<sup>41, 43, 44</sup>. Despite these compelling biomarker data, the role of GDF15 in cardiovascular biology is unknown.

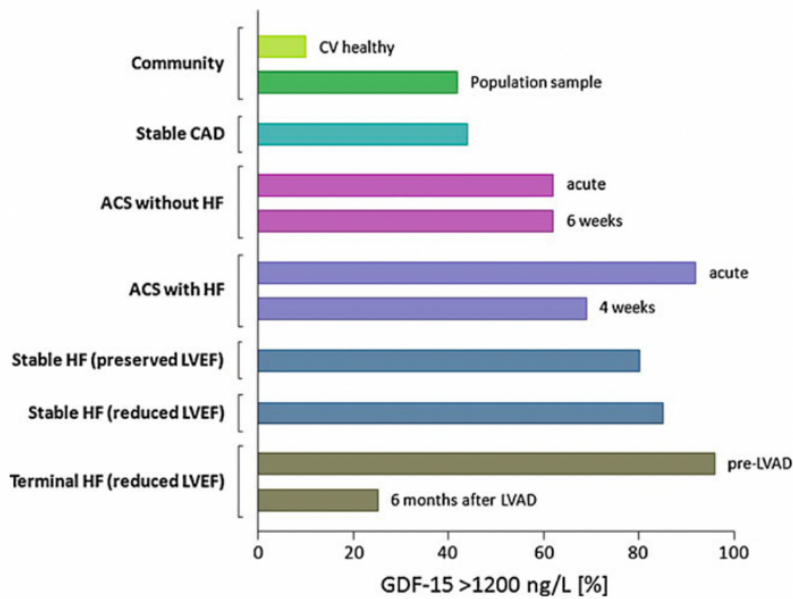


**Figure 7. GDF15 as a biomarker in numerous cardiovascular diseases.** Percent of population with elevated GDF15 levels (upper threshold: 1,200 ng/L) in distinct populations ranging from healthy individuals to patients experiencing end stage HF. CV= cardiovascular; CAD= coronary artery disease; ACS= acute coronary syndrome; LVEF= left ventricular ejection fraction; LVAD= left ventricular assist device. (Wollert et al., 2012).

Mouse models have provided limited insight into the function of GDF15 in heart disease. Transverse aortic constriction (TAC) is an experimental technique whereby a ligature is surgically placed around the aorta to narrow its luminal diameter. This creates an acute pressure overload on the heart that leads to LV hypertrophy (thickening of the heart muscle), and eventually LV dilation and HF. Using TAC in mice that either overexpress GDF15 or had GDF15 knocked out (KO) suggested a protective effect: overexpression was associated with less hypertrophy and HF while KO mice developed more severe HF than wild type mice<sup>46</sup>. However, the mechanism for this effect was not defined. Similarly, when subjected to experimental MI, GDF15 KO mice have larger infarct size and lower survival<sup>47</sup>. Interestingly, in this setting GDF15 exerted its protective effect by enhancing chemokine-activated leukocyte arrest on the endothelium, which promotes monocyte/macrophage transmigration into the heart, a critical first step in the healing process after an acute MI<sup>48</sup>.

TAC and MI models are somewhat artificial models of HF. Both are conducted in juvenile or adolescent mice, and both are acute methods to induce HF. This is far from the normal progression of HF in humans, which is a chronic disease that progresses over many years. Further, as noted above, the protective effect of GDF15 after MI occurs via an extra-cardiac mechanism (altered leukocyte recruitment). Hence, the biologic role of GDF15 in chronic HF remains unclear.

### PLN<sup>R9C</sup> Mice Models

Our lab utilizes a genetic mouse model of HF with a mutation in the phospholamban (*Pln*) gene<sup>49</sup>. Specifically, these mice carry a missense mutation at residue 9 that changes Arg to Cys (R9C). In humans, this mutation induces progressive DCM and HF in early adult life with all patients dying or receiving heart transplant by age ~40<sup>49-51</sup>. This mutation causes a hallmark

molecular feature of HF, which is altered calcium regulation in cardiomyocytes. PLN regulates the cardiomyocyte sarcoplasmic/endoplasmic reticulum calcium adenosine triphosphatase (SERCA2a) pump that is essential to normal cardiomyocyte calcium cycling. PLN<sup>R9C</sup> mice mimic human disease with a lengthy latent phase; they have no overt phenotypic features of DCM before 10-weeks of age (we call this the “preDCM” phase). However, between 12-20 weeks of age, they develop profound and progressive DCM that ultimately leads to symptomatic HF and premature death by ~25 weeks of age.

Our PLN<sup>R9C</sup> mouse model showcases several pathophysiological features of DCM and HF. These models have dilated ventricles, lower cardiac contractility, and increased cardiac fibrosis (Figure 8). Furthermore, not only do these PLN<sup>R9C</sup> mice develop HF, they also develop cardiac cachexia, as evidenced by overall weight loss and reduced fat and muscle mass in PLN<sup>R9C</sup> vs. age-matched wild type (WT) mice (Figure 9). These data identify the PLN<sup>R9C</sup> mouse model as a good model in which to study cachexia.

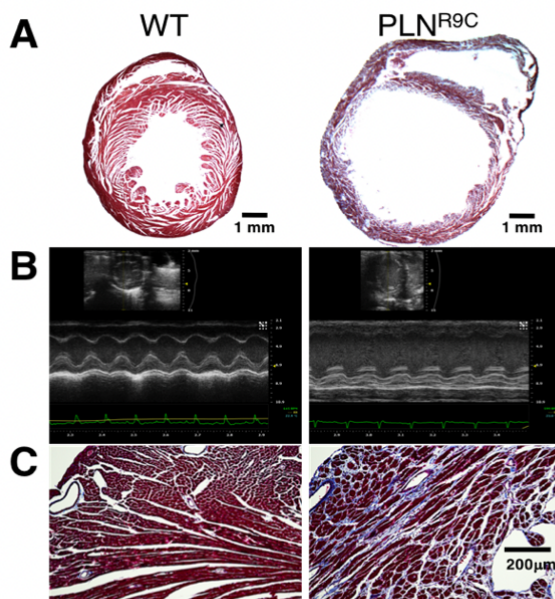


**Figure 8. PLN<sup>R9C/+</sup> mice develop hallmark features of HF.** (A) PLN<sup>R9C/+</sup> mice show LV dilation as seen by the increased size of the LV cavity in these whole mount heart sections. (B) Echocardiography (ultrasound imaging of the heart) shows reduced cardiac contraction and function in PLN<sup>R9C/+</sup> models. This can be seen via greater amplitude of waves in the right panel. (C) Severe fibrosis in PLN<sup>R9C/+</sup> heart tissue shown by the blue Masson trichrome staining. Increased levels of collagen types 1 and 3 are speculated in the PLN<sup>R9C/+</sup> models. Courtesy of Da Young Lee.

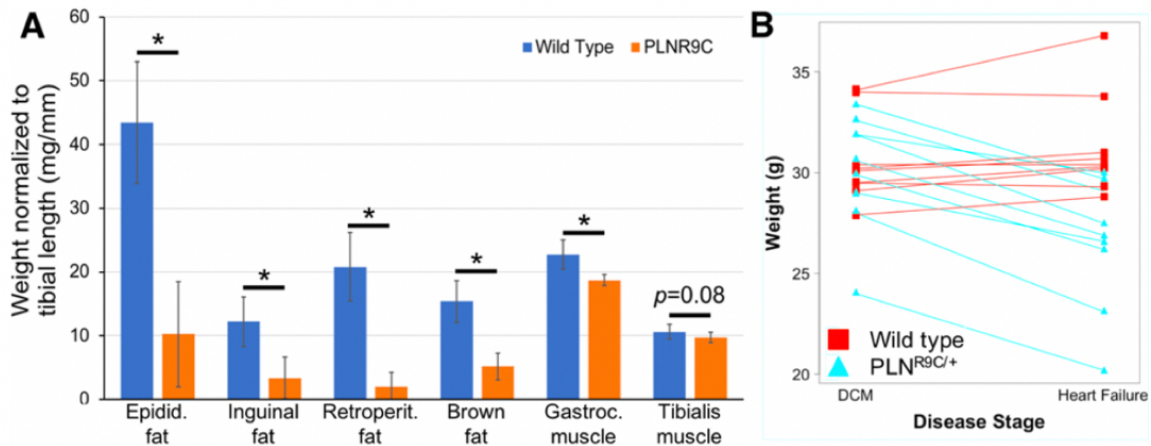


**Figure 9. Cardiac cachexia is present in PLN<sup>R9C/+</sup> mice models.** (A) Fat and muscle tissues were weighed from PLN<sup>R9C/+</sup> and WT mice (\*p<0.05, n=10). (B) Weight loss observed in PLN<sup>R9C/+</sup> mice models from the DCM stage to HF (p<0.05, n=10). (Burke et al., 2016).

To assess changes in gene transcription at different stages of disease in PLN<sup>R9C/+</sup> mice, our lab previously performed high-throughput next-generation RNA-sequencing (RNA-seq). Among other changes that revealed a marked increase in inflammatory gene network activation, we found a ~40-fold upregulation of *Gdf15* mRNA in the cardiomyocytes of failing PLN<sup>R9C/+</sup> hearts<sup>52</sup>. To explore whether *Gdf15* was upregulated in other forms of cardiomyopathy, we used publicly available genomic data from the NCBI's gene expression omnibus (GEO) database and found that upregulation of *Gdf15* was common to other mouse HF models (Table 3). However, the biological effect of GDF15 has not been studied specifically in HF. Because of this knowledge gap, no molecular mechanisms have been characterized that comprehensively associate GDF15 with cachexia. Therefore, our hypothesis is that **GDF15 is a myocardial-derived hormone that causes anorexia and cardiac cachexia.**

Table 3. Model	Fold Change	Method
Genetic DCM	N. R.	Microarray
MI & I/R	10-20	Microarray
Genetic HCM	2.7	RNA-seq
Genetic DCM	26	RNA-seq
Genetic DCM	30-40	RNA-seq
TAC	15	RNA-seq
MI	13	RNA-seq
MI	9.2	RNA-seq
Genetic DCM	35	RNA-seq

DCM=dilated cardiomyopathy; MI=myocardial infarction; I/R= ischemia/reperfusion; HCM= hypertrophic cardiomyopathy; TAC= thoracic aortic constriction; N.R.= fold change not reported, but significantly elevated

## **METHODS**

**Mouse Models:** To study the role of GDF15 in HF, we have obtained a *Gdf15* knock-out KO mouse model. This floxed GDF15 allele is a whole body, constitutive KO. *Gdf15* KO mice were obtained in the C57BL/6 genetic background. These mice were crossed for 10 generations to FVB mice to develop a congenic strain with the floxed GDF15 allele in the FVB genetic background. We then obtained  $Pln^{R9C/+}$  mice in the FVB background and crossed the *Gdf15* KO mice with the congenic strain (Figure 10) to produce the following 4 experimental groups: (1)  $Pln^{+/+}-Gdf15^{+/+}$  - these are wild type (WT) mice; (2)  $Pln^{+/+}-Gdf15^{-/-}$  - WT mice lacking *Gdf15*;

(3)  $Pln^{R9C/+}-Gdf15^{+/+}$  - DCM mice that express  $Gdf15$ ; (4)  $Pln^{R9C/+}-Gdf15^{-/-}$  - DCM mice lacking  $Gdf15$  (Table 4).

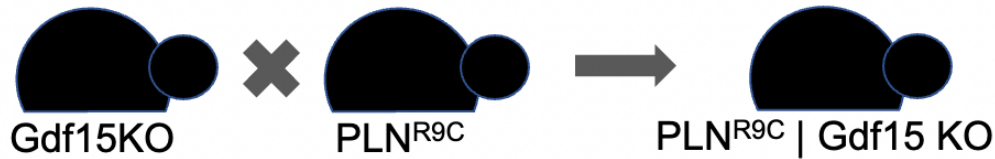


**Figure 10. Gdf15 KO mice crossed with PLN<sup>R9C</sup> mice create our main experimental group:  $Pln^{R9C/+}-Gdf15^{-/-}$ .**

Table 4. Pln-Gdf15 KO Mouse Model	
Mouse genotype	Usage
$Pln^{+/+}-Gdf15^{+/+}$	WT mice; baseline comparator for all groups
$Pln^{R9C}-Gdf15^{+/+}$	DCM mice with WT $Gdf15$ alleles; comparable to previously published data on the PLN <sup>R9C</sup> model
$Pln^{+/+}-Gdf15^{-/-}$	$Gdf15$ -null mice; will define the effect of $Gdf15$ KO in otherwise normal mice
$Pln^{R9C}-Gdf15^{-/-}$	DCM mice that are $Gdf15$ -null; the primary experimental study group

Courtesy of Da Young Lee

Sample Procurement: Mice were anesthetized with 2% isoflurane mixed with oxygen using a vaporizer (VetEquip). Then, hearts were exposed by midline thoracotomy and extracted, resulting in their death. Serum was taken via a direct cardiac puncture. Tissue (ex. fat, muscle, etc) was then dissected from these mice. The heart samples were washed in PBS buffer to remove any bodily fluids, and only the LV tissue was retained. RIPA buffer was utilized to extract protein from LV tissue and serum. Fat pads and muscle tissue were weighed. Tibia length was measured in order to normalize the fat, muscle, and body weight as well as food intake.

RNA extraction: I extracted total RNA from 10 types of organ tissues at 10- and 22-weeks of age

using TRIzol reagent. When extracting RNA from 10-week old fat tissue, we obtained poor quality control results on serial experiments. Therefore, to isolate high-quality RNA from fat at 10-weeks of age, we utilized Qiagen's RNeasy lipid tissue mini kit. RNA was quantified using a Nanodrop spectrometer. Isolated RNA was then used for Q-PCR or sent for RNA-seq as detailed below.

Quantitative-PCR: I isolated RNA from heart, lung, spleen, brain, kidney, liver, muscle, fat, small intestine, and colon tissue and then performed Q-PCR as follows. Total RNA was quantified using a Nanodrop spectrometer. The RNA was converted to cDNA via the SuperScript III First-strand Synthesis System (Invitrogen). Q-PCR was performed using the BioRad QX200 digital droplet PCR platform with a FAM-labeled TaqMan probe targeting mouse Gdf15. We used a VIC (*Aequora victoria* Green Fluorescent Protein)-labeled 18s rRNA probe for normalization. A reaction mixture was created with the following: 1 µl of cDNA solution, 12.5 µl of digital PCR™ Supermix (Bio-Rad), 1.25 µl of probe (Gdf15 or 18s rRNA), and 10.25 µl of DEPC H<sub>2</sub>O. This solution was loaded into a 96-well PCR plate with 70 µl of QX200 Droplet Generation oil (Bio-Rad) and then placed into QX200 Droplet Generator (Bio-Rad). Droplets were then transferred to a new 96-well PCR plate and the plate was sealed with foil using a BioRad plate sealer. PCR amplification was performed on a thermal cycler at 95°C for 10 min, followed by 40 cycles of 95°C for 30 seconds and 60°C for 1 min, 1 cycle of 98°C for 10 min, and finally ending at 4°C. The plate was then loaded into the QX200 Droplet Reader (Bio-Rad). The number of positive droplets were recorded and then normalized to 18sRNA. All tests were performed in duplicate (technical replicates).

ELISA: A Quantikine ELISA Kit (Mouse/Rat GDF-15 immunoassay) was used according to the

manufacturer's directions. In brief: samples of LV lysate and serum were first incubated in GDF15 antibody-coated microplates for 2 hours then washed and incubated with GDF15 antibody conjugate for 2 hours. After washing, color reagent was added and the plate was incubated for 30 min. The microplate reader was set to 450 nm and 570 nm. Then, a standard curve using Calibrator Diluent RD5P diluted at 1:5 (500 pg/mL standard serving as the high standard) was generated. Triplicates were performed.

Dual energy X-ray absorptiometry (DEXA): Isoflurane was used to anesthetize 24-week old mice. Kubtec Scientific Parameter Cabinet X-ray System was used to quantify total, fat, and lean body mass. Mouse tibia length was measured.

Food Intake: A subset of mice were individually housed to track food intake. Beginning at 10-weeks of age, food remaining in the cage was weighed weekly. When mice had evidence for overt HF, they were sacrificed along with a *Gdf15* genotype-matched WT mouse. Food intake over the final 3 weeks of life was assessed.

Survival: In our lab's past experience, once overt HF is present, PLN<sup>R9C</sup> mice typically die within 2-3 days. Hence, we assessed survival free from overt HF in *Pln*<sup>R9C/+</sup>-*Gdf15*<sup>+/+</sup> and *Pln*<sup>R9C/+</sup>-*Gdf15*<sup>-/-</sup> mice. As per IACUC regulations, at the onset of symptoms, mice were sacrificed in the survival analysis.

Echocardiography: Mice were anesthetized with isoflurane and then secured to a Vevo Mouse Handling Table (VisualSonics Inc.). Chest hair was removed with depilatory cream and 2-dimensional and M-mode echocardiography was performed using a Vevo 770 High-Resolution In Vivo Micro-Imaging System with RMV 707B scan-head (VisualSonics Inc.). The following parameters were measured: left ventricular end diastolic diameter (LVEDD), left ventricular wall thickness (LVWT), fractional shortening (FS), and left ventricular end systolic diameter (LVESD). LVEDD is the size of the LV chamber when the heart is relaxed (end diastole) after contraction, and is a measure of LV structure and chamber dilation. LVESD is size of the LV chamber at peak contraction (end systole) and is a measure of LV contractile function. LVWT is the combined thickness of the LV septal and posterior walls at end diastole; this is also a measure of LV structure. FS is a measure of cardiac contractility and showcases how close the cardiac walls come together during a heartbeat.

Histochemistry: After harvesting hearts as detailed above, hearts were placed in PBS to removed excess blood. Hearts were then fixed in buffered 4% paraformaldehyde (pH 7.4) overnight followed by 2 10-minute washes with PBS. Hearts were embedded in paraffin and 5  $\mu\text{m}$  sections were cut by the Winship histology core facility at a variable number of levels that were 75  $\mu\text{m}$  apart from apex to base such that the representative regions of entire heart were examined. Picrosirius red staining was used to identify LV fibrosis (explain protocol). Finally, slides were imaged using a Hamamatsu NanoZoomer SQ, and fibrosis was quantified by Image J (NIH).

RNA-sequencing: In a separate cohort of mice, white fat tissue was extracted for RNA collection. Sample purity was confirmed using an Agilent 4200 TapeStation by the core facility

and RNA-seq was performed using 150 bp paired end sequencing on a NovaSeq 6000. QC was performed on all samples by the core facility and differential gene expression was analyzed using the DEseq2 platform<sup>53</sup>. The gene ontology tool DAVID was used to identify gene ontology terms and pathways that were enriched among differentially expressed genes.

Statistics: Data are presented as mean  $\pm$  SD for normally distributed data. For QPCR and ELISA, between-groups differences were calculated using a 2-tailed Student's *t* test; *P* values less than 0.05 were considered significant. Kaplan Meier survival plot was used to measure survival spans of mice models. Log rank tests were used to compare the statistical significance of survival of the two experimental groups.

## **RESULTS**

To address our hypothesis, our lab has previously characterized the phenotype of the PLN<sup>R9C</sup>-Gdf15 KO model. *Pln*<sup>R9C/+</sup>-*Gdf15*<sup>+/+</sup> mice had significant fat and muscle wasting when compared to all other experimental groups (Figure 11A.  $p < 0.01$  for all comparisons,  $n = 19/\text{genotype}$ , 9B.  $p < 0.001$  for gastrocnemius and  $p = 0.001$  for tibialis,  $n = 19/\text{genotype}$ ). This suggests that GDF15 is a driver of cachexia in HF. To confirm these results, we performed DEXA scanning to quantify fat and muscle mass (Figure 11). We found significant wasting of fat mass in *Pln*<sup>+/+</sup>-*Gdf15*<sup>+/+</sup> mice when compared to *Pln*<sup>+/+</sup>-*Gdf15*<sup>-/-</sup> mice ( $p < 0.05$ ). Importantly, fat mass was preserved in *Pln*<sup>R9C/+</sup>-*Gdf15*<sup>-/-</sup> mice versus *Pln*<sup>+/+</sup>-*Gdf15*<sup>+/+</sup> mice ( $p < 0.05$ ) and was not significantly different than WT. By DEXA, lean mass was not found to be different. However, edema, is a measured component of lean mass via DEXA scanning. Edema is a cardinal feature

of HF and it develops in  $PLN^{R9C}$  mice with advanced disease. Hence, this neutral result is likely due to the excess edema in  $PLN^{R9C}$ -positive mice.

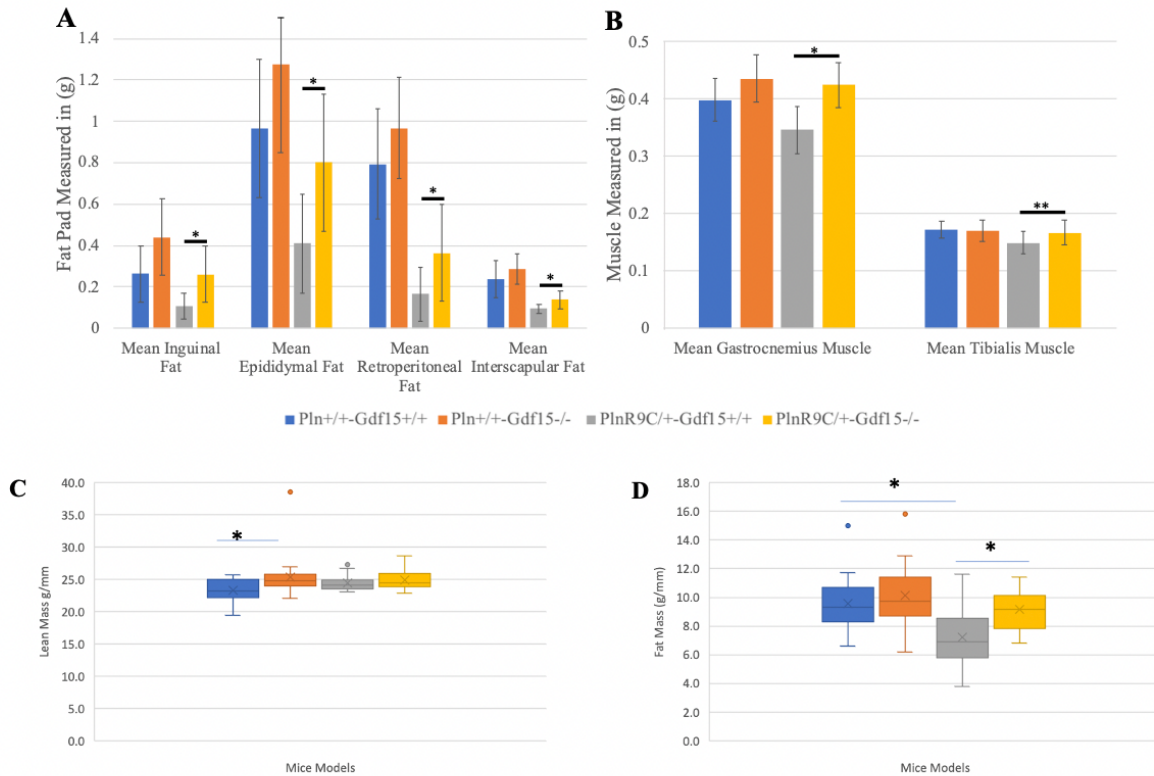


**Figure 11. Suggested cachexia in mice models with elevated GDF15 levels.** (A,B) Significant fat and muscle wasting was seen in our experimental group  $Pln^{R9C/+}-Gdf15^{+/+}$ . ( $p < 0.01$ ) (C,D) DXA screenings showcase significant fat mass wasting in  $Pln^{R9C/+}-Gdf15^{+/+}$  mice. ( $p < 0.05$ ). Courtesy of Da Young Lee.

Given the recently established effect of GDF15 on food intake, we also assessed food intake. We found that  $Pln^{R9C/+}-Gdf15^{+/+}$  mice had significantly reduced food intake when compared to other groups ( $p < 0.05$ ). Importantly,  $Pln^{R9C/+}-Gdf15^{-/-}$  mice had significantly higher food intake than  $Pln^{R9C/+}-Gdf15^{+/+}$  ( $p < 0.05$ ), signifying that GDF15 levels play a role in food intake in HF. This observation suggests that one possible mechanism of cardiac cachexia in HF is anorexia.

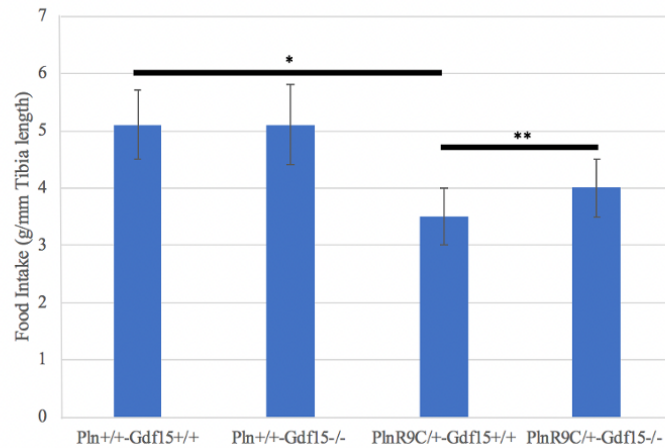


**Figure 12. GDF15 alters food intake.** Food intake in  $Pln^{R9C/+}$ - $Gdf15^{+/+}$  models was significantly reduced (\*\* $p < 0.05$ ), suggesting anorexia as one of the mechanisms that causes cachexia. Courtesy of Da Young Lee.

Finally, survival was assessed (Figure 13). We found that  $Pln^{R9C/+}$ - $Gdf15^{-/-}$  mice lived 15% longer ( $29 \pm 3$  weeks vs.  $25 \pm 3$  weeks; log-rank  $p < 0.01$ ,  $n = 32$  mice/ $Pln^{R9C/+}$ - $Gdf15^{+/+}$ ,  $n = 39$  mice/ $Pln^{R9C/+}$ - $Gdf15^{-/-}$ ). This suggests that elevated GDF15 levels contribute to higher mortality rates as DCM progresses.

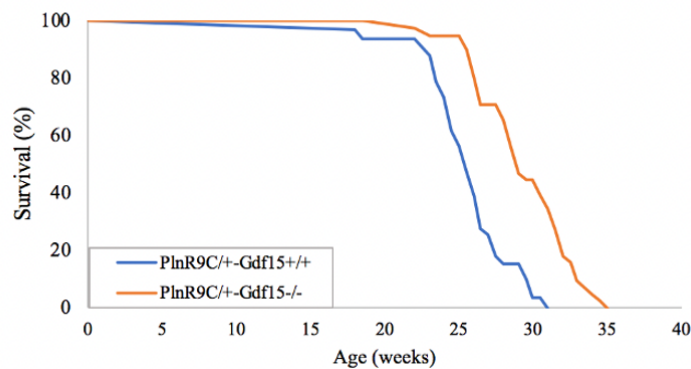


**Figure 13. GDF15 levels affect mortality rate.** Kaplan Meier plot of survival of GDF15 WT and KO mice model groups ( $n = 32$  mice/ $Pln^{R9C/+}$ - $Gdf15^{+/+}$ ;  $n = 39$  mice/ $Pln^{R9C/+}$ - $Gdf15^{-/-}$ , log-rank test,  $p < 0.01$ ). Courtesy of Da Young Lee.

Next, we assessed the cardiac phenotype of these mice to further our understanding of the interaction between HF and GDF15. Echocardiography was performed on our 4 experimental groups from week 10 to week 22 (Figure 14).  $Pln^{R9C}$  mice developed DCM when compared to WT mice: progressive LV dilation, LV wall thinning, and reduced LV systolic function was present in the former group (LVEDD:  $4.5 \pm 0.4$  mm vs.  $3.2 \pm 0.3$  mm; LVWT:  $1.3 \pm 0.2$  mm vs.  $1.6 \pm 0.2$  mm; FS:  $17\% \pm 5\%$  vs.  $45\% \pm 7\%$ ; LVESD:  $3.8 \pm 0.6$  mm vs.  $1.8 \pm 0.3$  mm;  $n=10 Pln^{+/-} Gdf15^{+/+}$ ,  $n=17 Pln^{R9C/+} Gdf15^{+/+}$ ;  $p<0.001$  for all). However, when comparing  $Pln^{+/-} Gdf15^{-/-}$  to  $Pln^{+/+} Gdf15^{+/+}$  mice, no differences were identified with  $Gdf15$  KO (LVEDD:  $4.2 \pm 0.5$  mm vs.  $4.5 \pm 0.4$  mm,  $p=0.22$ ; LVWT:  $1.3 \pm 0.3$  mm vs.  $1.3 \pm 0.2$  mm,  $p=0.71$ ; FS:  $22\% \pm 7\%$  vs.  $16\% \pm 6\%$ ,  $p=0.48$ ; LVESD:  $3.4 \pm 0.6$  mm vs.  $3.8 \pm 0.6$  mm,  $p=0.38$ ;  $n=17 Pln^{R9C} Gdf15^{+/+}$ ,  $n=18 Pln^{R9C/+} Gdf15^{-/-}$ ).

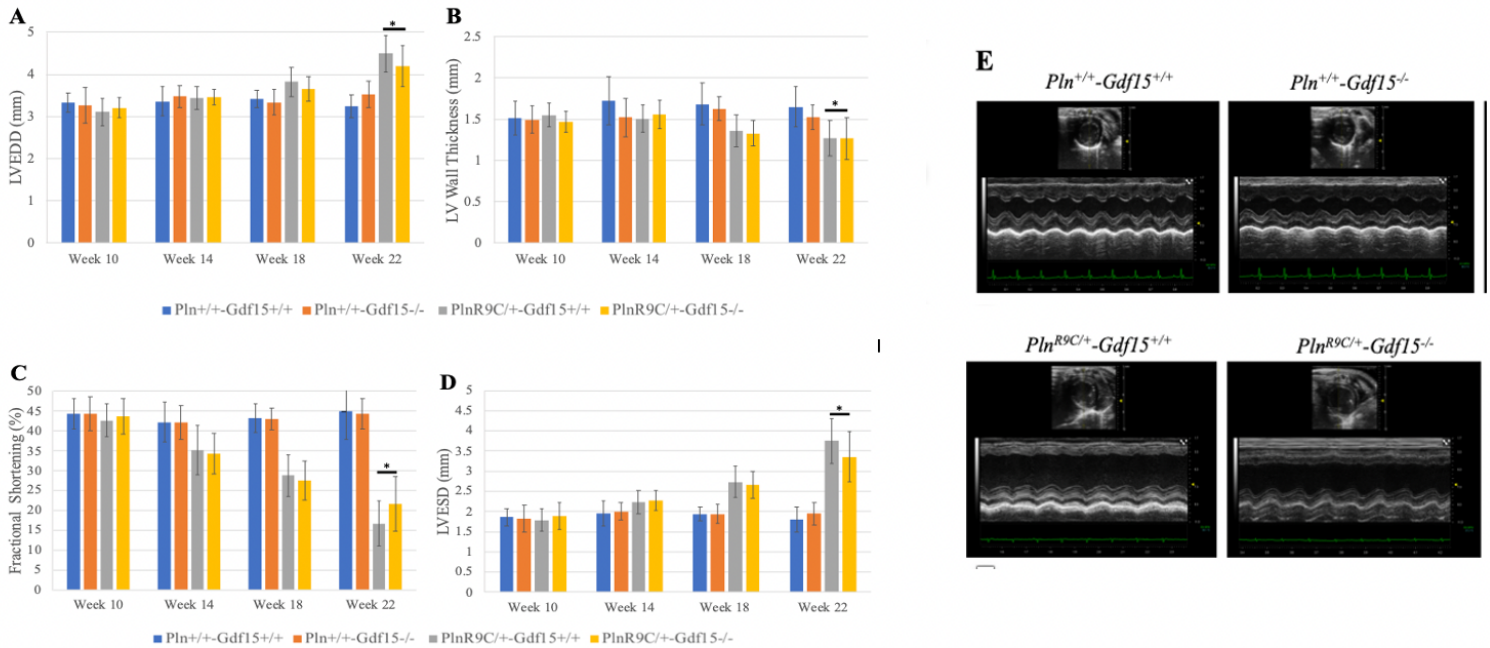


**Figure 14. GDF15 does not alter cardiac morphology or function.** (A-D) Cardiac morphology parameters were measured longitudinally in mice models from 10 weeks to 22 weeks. No significant difference was observed in GDF15 KO models with the  $PLN^{R9C}$  mutation. (E) Echocardiography images photographing heartbeats that are associated with mice model hearts in panels A-D. No contractility differences in  $PLN^{R9C}$  models are shown. Similarly, no cardiac contractility differences in WT PLN models are seen. (\*p=n.s. for all analyses, n=10/ $Pln^{+/+}-Gdf15^{+/+}$ , n=11/ $Pln^{+/+}-Gdf15^{-/-}$ ; n=17/ $Pln^{R9C/+}-Gdf15^{+/+}$ , n=18/ $Pln^{R9C/+}-Gdf15^{-/-}$ ; ANOVA).

We also assessed cardiac fibrosis, another hallmark feature of HF, using picrosirius red stained LV tissue sections (Figure 15). When comparing our  $PLN^{R9C/+}-Gdf15^{+/+}$  models with  $Pln^{+/+}-Gdf15^{+/+}$  models, there was a significant increase in fibrosis in the latter group (21.3% vs. 1.4%  $Pln^{+/+}-Gdf15^{+/+}$ ; 15.2% relative increase; p=0.001; n=3/genotype). However, although our  $PLN^{R9C/+}-Gdf15^{+/+}$  and  $PLN^{R9C/+}-Gdf15^{-/-}$  models had elevated fibrosis levels with a statistical significance, we think there is no biologically significant difference between the two (18.2% vs. 21.3%, p=0.001). This suggests that GDF15 does not impact cardiac morphology or function.

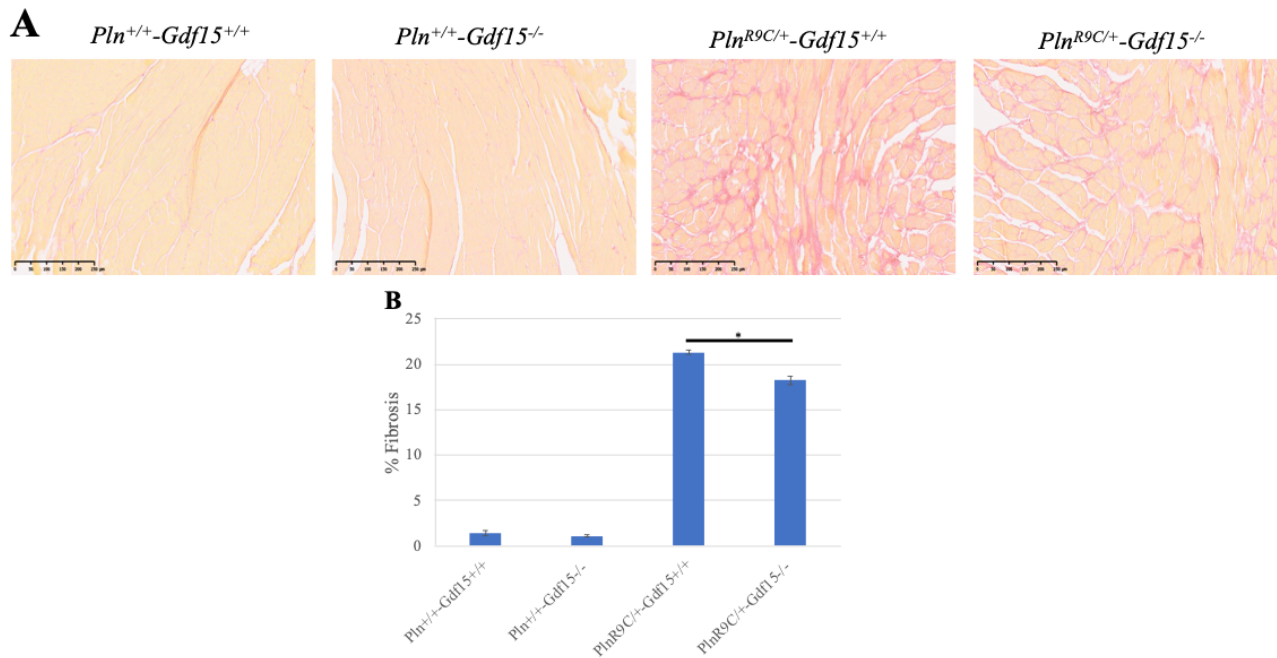


**Figure 15. PLN<sup>R9C/+</sup> mice develop fibrosis regardless of GDF15 genotype.** (A) Representative images of picrosirius red stained heart tissue by genotype cells using a Hamamatsu NanoZoomer SQ. Red staining identifies collagen-rich areas of the heart tissue, yellow staining predominantly shows cardiac muscle cells. Scale bar = 250 um. (B) Quantified fibrosis from the 4 experimental groups at the age of 26 weeks (\*p=0.001). Courtesy of Da Young Lee.

## My Specific Aims

### *GDF15 is only increased in the failing heart.*

My first aim was to establish that the upregulation in *Gdf15* mRNA in PLN<sup>R9C</sup> mice is (1) specific for the heart; (2) correlates with increased GDF15 protein in the heart; and (3) translates to elevated circulating levels of GDF15 compared to WT mice. I performed QPCR on mRNA from 10 tissue types in preDCM PLN<sup>R9C/+</sup> mice at 8 weeks of age, and mice with HF at 22 weeks of age, along with age-matched WT mice. In preDCM mice, *Gdf15* mRNA increased ~10.6-fold in the LV tissue (p=0.012) in PLN<sup>R9C</sup> mice compared to WT. In mice with DCM, there was a 48.4-fold increase in cardiac *Gdf15* mRNA levels compared to WT (p<0.001). In all other tissue types, *Gdf15* levels were low and did not change significantly when comparing PLN<sup>R9C</sup> to WT

mice at different time points. These data demonstrate that *Gdf15* is increased specifically and exclusively in the failing heart.

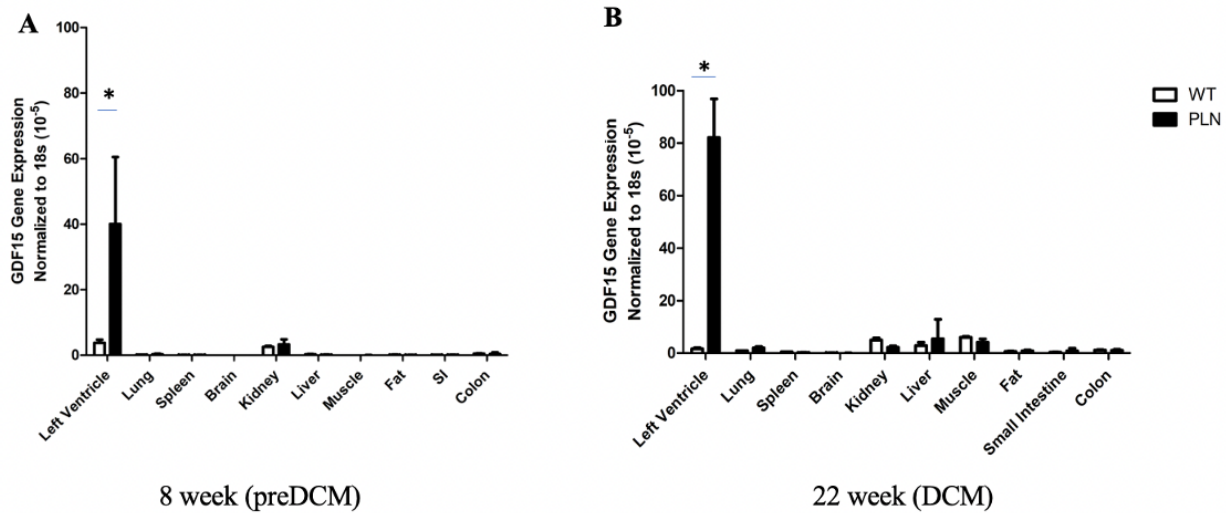


**Figure 16. *Gdf15* mRNA levels are upregulated in PLN<sup>R9C/+</sup> hearts.** (A) In 8-week mice, there is no significant upregulation of *Gdf15* mRNA levels between WT and PLN<sup>R9C/+</sup> mice. No significant increase observed in other tissue types. (\*p=.01, n=4) (B) In 22-week mice, there is a significant increase in *Gdf15* mRNA levels, suggesting an upregulation of *Gdf15* levels when DCM occurs. No significant increase observed in other tissue types. (\*p=0.001, n=4).

Next, to confirm that GDF15 protein levels increase in the heart commensurate with the increased mRNA, I performed ELISA to quantify GDF15 protein levels in LV tissue in preDCM and DCM mice, and age-matched WT (Figure 17). I found a small but significant increase in GDF15 protein in LV tissue in preDCM PLN<sup>R9C</sup> mice (9pg/mg LV tissue in PLN<sup>R9C</sup> vs. undetectable in WT LV tissue, n=4/genotype; p=0.011). In DCM mice, there was a marked upregulation of GDF15 protein levels in PLN<sup>R9C</sup> compared to WT and compared to PLN<sup>R9C</sup> preDCM hearts. (98pg/mg LV tissue, 54-fold increase vs. WT, n=4/genotype, p=0.002).

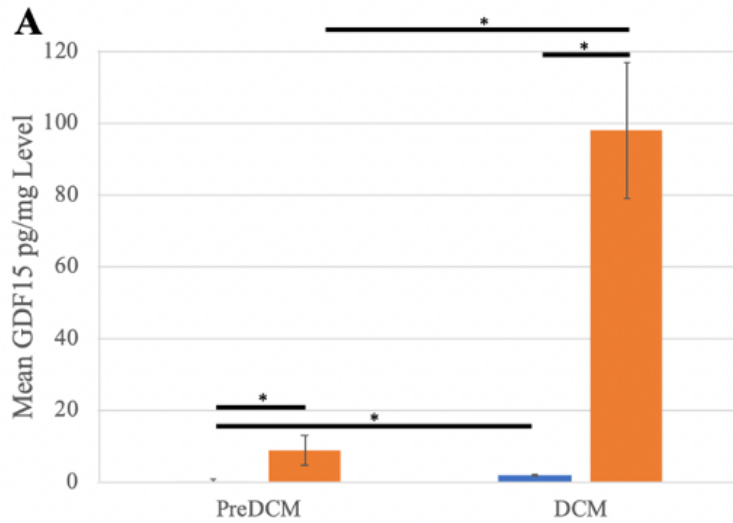


**Figure 17. GDF15 protein levels are upregulated in PLN<sup>R9C</sup> LV tissue.** (A) A significant increase in GDF15 protein levels was observed in PLN<sup>R9C</sup> LV tissue preDCM and in DCM. (\*p<0.05)

Finally, I examined circulating GDF15 levels in the serum (Figure 18). Again, I found a small but significant upregulation in preDCM PLN<sup>R9C/+</sup> mice (1.4 fold increase, p=0.045). In mice with DCM, I noted a much greater increase in circulating GDF15, with a significant 6.1-fold increase in PLN<sup>R9C/+</sup> mice (p<0.001). Collectively, these data demonstrate that GDF15 is specifically produced by the failing heart in greater quantities as the disease progresses and is secreted into the blood stream.

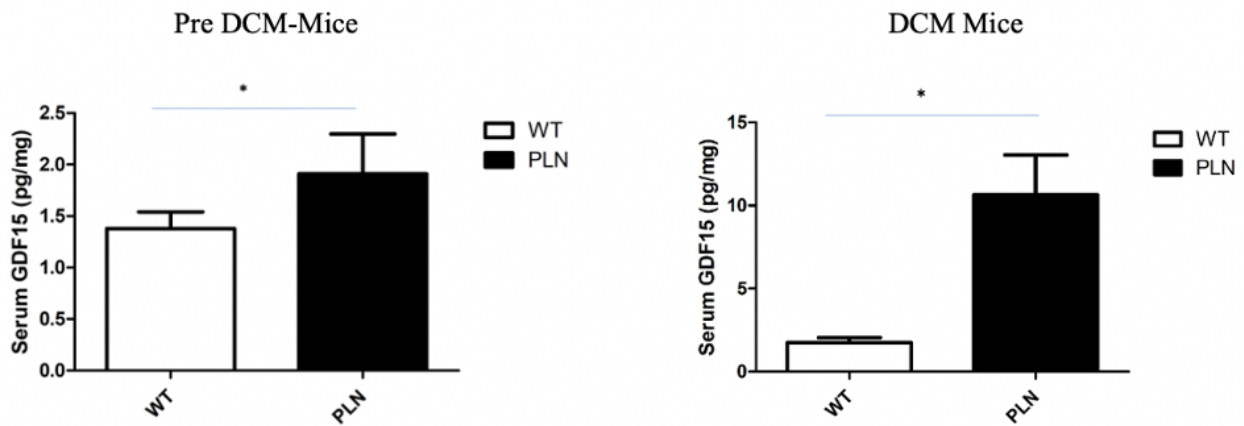


**Figure 18. GDF15 protein levels are upregulated in PLN<sup>R9C</sup> bloodstream.** A marked increased in circulating GDF15 protein levels was observed in PLN<sup>R9C</sup> LV tissue in both preDCM (p=0.045) and DCM models. (p=0.001)

### *GDF15 triggers peripheral metabolic changes.*

My second aim was to establish a correlation between GDF15 and peripheral metabolic changes in our mice models. I collected fat tissue from 10- and 22-weeks old mice and extracted total RNA. Then, I sent the RNA to the Yerkes Genomics Core for RNA-seq analysis. From the RNA-seq results, I performed gene ontology analysis using a web tool called DAVID. I first sorted all genes based on which ones were differentially regulated. Next, I uploaded them into the platform. Firstly, there was no differential change in lipid and fat metabolic processes in 10-week mice in any experimental group. Furthermore, in 10-week mice with DCM, I found that there was no difference in the lipid and fat metabolic processes regardless of the GDF15 genotype i.e. no difference between our *Pln*<sup>+/+</sup>-*Gdf15*<sup>+/+</sup> and *Pln*<sup>+/+</sup>-*Gdf15*<sup>-/-</sup>. This suggests that when GDF15 is not expressed in the body, there is no systemic effect of this molecule.

However, there was a significant downregulation of the genes involved in lipid and fat metabolic pathways when comparing our 22-week old *Pln*<sup>R9C/+</sup>-*Gdf15*<sup>+/+</sup> and *Pln*<sup>+/+</sup>-*Gdf15*<sup>+/+</sup>

mice models ( $p < 0.05$  for all genes listed). Furthermore, when looking at the GO terms for these lipid pathways, these genes were enriched in the *Pln*<sup>R9C/+</sup>-*Gdf15*<sup>+/+</sup> versus *Pln*<sup>+/+</sup>-*Gdf15*<sup>+/+</sup> mice models, meaning that the amount of RNA molecules for these genes differed significantly between the two groups. This suggests that when HF occurs in mice models, there is an alteration of metabolic pathways due to the nature of this syndrome.

Lastly, when comparing our *Pln*<sup>R9C/+</sup>-*Gdf15*<sup>-/-</sup> and *Pln*<sup>+/+</sup>-*Gdf15*<sup>+/+</sup> mice models, we saw no significant change in the genes associated with these metabolic pathways ( $p > 0.05$  for all genes studied).

22 Weeks	PLN/KO vs WT/WT	PLN/KO vs WT/WT	PLN/WT vs WT/WT	PLN/WT vs WT/WT
	Fold Change	P VALUE	Fold Change	P VALUE
Apoa2	-4.990361762	0.208622799	-7.302582439	1.79168E-07
Apoc3	-3.629548322	0.987810399	-5.638679142	0.0332875
Apon	-4.830318176	0.319700447	-7.292034577	0.021680461
<b>Cyp2c29</b>	-6.021301011	0.208622799	-6.864303104	0.022655228
<b>Cyp2c70</b>	-3.120990161	0.200881008	-3.295722078	0.0332875
<b>Cyp2d9</b>	-2.009781696	0.999930156	-5.006638787	0.008708959
Cyp3a11	-4.82122931	0.580422305	-6.348880194	0.032628589
Cyp3a25	-4.843465258	0.18240781	-8.110303047	0.002026302
<b>Fabp1</b>	-5.382819451	0.275426962	-6.067399003	0.032173049
<b>Lep</b>	-0.305418116	0.999930156	-0.815604752	0.047972324
Mogat2	-0.334468571	0.999930156	-1.832903534	0.002190648
<b>Scd2</b>	-0.166252256	0.999930156	-1.019428274	0.033849447

**Figure 19. GDF15 alters fat metabolism in DCM mice models.** The following genes are significantly downregulated in our *Pln*<sup>R9C/+</sup>-*Gdf15*<sup>+/+</sup> versus *Pln*<sup>+/+</sup>-*Gdf15*<sup>+/+</sup> mice models, therefore suggesting an alteration of the associated metabolic pathways with these genes. However, there is no significant difference observed when comparing *Pln*<sup>R9C/+</sup>-*Gdf15*<sup>-/-</sup> versus *Pln*<sup>+/+</sup>-*Gdf15*<sup>+/+</sup>, therefore suggesting that only when GDF15 is present that these genes are significantly altered.

## DISCUSSION

Cardiac cachexia is a potentially catastrophic consequence of HF. In this project, I have identified GDF15 as a potential cardiac hormone that is secreted specifically from the heart and causes cardiac cachexia in HF. I examined gene expression in different organ tissues to confirm

that GDF15 is secreted specifically from the failing heart and has upregulated circulating levels. Using a genetic mouse model, our lab has observed that GDF15 KO reduced cardiac cachexia and increased food intake in mice with HF. An additional benefit seen in our GDF15 KO models is the increased survival rate when compared to GDF15 models. Surprisingly, this occurs in the absence of substantial changes in cardiac structure and function. Lastly, I have now demonstrated that fat metabolism is altered by GDF15, pointing to the systemic effects that this molecule may exhibit. The absence of GDF15 potentially restores the changes in lipid and fat metabolism. This can provide strong evidence that GDF15 plays a role in HF in PLN<sup>R9C</sup> mice as it alters fat metabolism, leading to excess lipolysis and cachexia. Collectively, these data suggest that GDF15 is a novel cardiac hormone.

Presently, BNP (brain-type natriuretic peptide) and ANP (atrial natriuretic peptide)<sup>54</sup> are the only known cardiac hormones. In response to HF, they are secreted to reduce arterial pressure and blood volume. Both bind to the cell receptor guanylyl cyclase to trigger a signaling cascade involving intracellular cGMP. Currently, a drug called Entresto is used in HF patients that targets these molecules. This drug is classified as an angiotensin receptor neprilysin inhibitor. By blocking neprilysin and angiotensin, angiotensin II and aldosterone release is blocked, thereby reducing the blood pressure and volume. This relieves the workload on the failing heart.

My data suggests that GDF15 is also a novel cardiac hormone, suggesting a new and previously unappreciated endocrine function for the heart. However, what distinguishes GDF15 in comparison to these two hormones is its specific binding to GFRAL and its upregulation in chronic stress. GDF15 having a completely different cell receptor expands the possibilities of drug developments as therapeutics can now target different cell receptors. Furthermore, GDF15

is unique in that it is only present in continuous and prolonged bodily stresses, an aspect that ANP and BNP do not have.

Cachexia is observed in a similarly morbid and chronic disease: cancer. Elevated GDF15 levels are also found in late stages of these diseases, and this molecule has been characterized as a tumor-derived activator of cachexia in certain types of cancer<sup>12</sup>. Aligning with past studies that have shown GDF15 to have systemic effects that cause anorexia<sup>12-15</sup>, I have established that GDF15 is associated with cardiac cachexia during HF. By measuring tissue weight and performing DEXA scanning, we were able to characterize differences in tissue composition with or without GDF15. We also found that GDF15 correlated directly with food intake, suggesting a possible causal role for anorexia in the cachexia observed in PLN<sup>R9C</sup> mice. Although we established that GDF15 does not affect cardiac morphology or function, there was a surprising increase in survival in GDF15 KO mice models when compared to our GDF15 WT models with HF. This suggests that the cachectic state has an impact on survival independent of any change in cardiac function, thereby increasing the importance of studying the association of GDF15 and cardiac cachexia.

Although cardiac cachexia is a deadly complication of HF, no therapeutic strategies have been developed to target this symptom. The pharmaceutical targeting of the GDF15-GFRAL axis can provide therapies for HF and cardiac cachexia. By identifying GDF15 as a novel hormone specifically secreted by the failing heart, we have a direct impact in this research realm as this hormone is a backbone of this mechanism. Some potential effective therapies include preventing the binding of GDF15 to the GFRAL receptor, so the body does not enter the cachectic state. Another potential drug could preemptively alter the GDF15 levels secreted from the failing heart to dampen the effects of cardiac cachexia. Given the massive possibilities of drugs pertaining to HF and cardiac cachexia, it is clear that our project's results can be a beneficial addition to the

pharma industry.

Our study has several strengths. First, the PLN mouse model undergoes progressive DCM leading to HF, which more closely mirrors the disease process in humans than other established mouse HF models such as TAC or MI. Previously published studies that suggested protective effects of GDF15 used TAC or MI<sup>46-48</sup>. The cardiovascular events in these studies are induced artificially with a sudden onset in otherwise normal adolescent mice. This causes a dissonance of age ranges studied in these mice models versus humans. Mice models are often in young age or adolescent years when these cardiovascular events are induced. This is out of norm for human patients as heart attacks and other significant cardiovascular events usually occur later in life. Therefore, our data are different because not only do we specifically study HF in our mice models, but we also recreate the slow progression of HF to account for the proper age range in mice. Also, the PLN mutation recapitulates a hallmark feature of HF in our mice models that also is present in humans: altered calcium signaling. Due to these differences in the mice models used between the studies and our project, the cardioprotective effects of GDF15 can be questioned in cardiac events and HF. Another strength of our study is the rigorous and temporal phenotyping that showcases the upregulation of GDF15 in later stages of diseases. We examined the mice models longitudinally as they developed progressive DCM, therefore allowing for a comprehensive association of GDF15 being upregulated only in chronic and continuous metabolic bodily stress. Lastly, the usage of RNA sequencing analysis further minimizes the bias when studying peripheral metabolic changes.

However, our study also has limitations as we have yet to identify a mechanism of action as to how GDF15 causes cachexia. One future aim to explore is the GDF15-GFRAL axis that regulates food intake. By further analyzing the high affinity and specific interactions between

GDF15 and the GFRAL-expressing neurons in the hindbrain, a systemic, noncardiac mechanism can be established that correlates with fat metabolism regulation<sup>17-20</sup>. We have obtained brain tissue from mice with HF. In collaboration with the Pederson lab (Emory Neurology) we will section these brains and use immunohistochemistry to co-localize activated neurons (c-Fos-positive cells) with GFRAL-expressing neurons in the brainstem, and to co-localize GFRAL and phosphorylated-ERK, which identifies cells with active Ret-signaling, a hallmark feature of GFRAL activation.

In our project, we have characterized GDF15 as a driver of cachexia secreted directly from the failing heart. This finding can provide novel treatments to treat the HF associated anorexia and cachexia. Potential avenues for research include understanding how GDF15 is upregulated in cardiomyocytes, further exploring the GDF15-GFRAL axis, and specifically studying a shift in cardiac metabolism. Despite these future explorations, our research provides a foundation for the next therapeutic drug of HF in hopes to lower the high mortality and morbidity associated with this deadly disease.

## **REFERENCES**

1. Yancy CW, Jessup M, Bozkurt B, Butler J, Casey DE, Jr., Drazner MH, Fonarow GC, Geraci SA, Horwich T, Januzzi JL, Johnson MR, Kasper EK, Levy WC, Masoudi FA, McBride PE, McMurray JJ, Mitchell JE, Peterson PN, Riegel B, Sam F, Stevenson LW, Tang WH, Tsai EJ, Wilkoff BL, American College of Cardiology F and American Heart Association Task Force on Practice G. 2013 ACCF/AHA guideline for the management of heart failure: a report of the American College of Cardiology Foundation/American Heart Association Task Force on Practice Guidelines. *J Am Coll Cardiol.* 2013;62:e147-239.
2. Virani SS, Alonso A, Benjamin EJ, Bittencourt MS, Callaway CW, Carson AP, Chamberlain AM, Chang AR, Cheng S, Delling FN, Djousse L, Elkind MSV, Ferguson JF, Fornage M, Khan SS, Kissela BM, Knutson KL, Kwan TW, Lackland DT, Lewis TT, Lichtman JH, Longenecker CT, Loop MS, Lutsey PL, Martin SS, Matsushita K, Moran AE, Mussolino ME, Perak AM, Rosamond WD, Roth GA, Sampson UKA, Satou GM, Schroeder EB, Shah SH, Shay CM, Spartano NL, Stokes A, Tirschwell DL, VanWagner LB, Tsao CW, American Heart Association Council on E, Prevention Statistics C and Stroke Statistics S. Heart Disease and Stroke Statistics-2020 Update: A Report From the American Heart Association. *Circulation.* 2020;141:e139-e596.
3. Tsao CW, Aday AW, Almarzooq ZI, Alonso A, Beaton AZ, Bittencourt MS, Boehme AK, Buxton AE, Carson AP, Commodore-Mensah Y, Elkind MSV, Evenson KR, Eze-Nliam C, Ferguson JF, Generoso G, Ho JE, Kalani R, Khan SS, Kissela BM, Knutson KL, Levine DA, Lewis TT, Liu J, Loop MS, Ma J, Mussolino ME, Navaneethan SD, Perak AM, Poudel R, Rezk-Hanna M, Roth GA, Schroeder EB, Shah SH, Thacker EL, VanWagner LB, Virani SS, Voecks

JH, Wang NY, Yaffe K and Martin SS. Heart Disease and Stroke Statistics-2022 Update: A Report From the American Heart Association. *Circulation*. 2022;145:e153-e639.

4. Hartupee J and Mann DL. Neurohormonal activation in heart failure with reduced ejection fraction. *Nat Rev Cardiol*. 2017;14:30-38.

5. Osborne C, Chaggar PS, Shaw SM and Williams SG. The renin-angiotensin-aldosterone system in heart failure for the non-specialist: the past, the present and the future. *Postgraduate Medical Journal*. 2017;93:29.

6. Bielecka-Dabrowa A, Ebner N, Dos Santos MR, Ishida J, Hasenfuss G and von Haehling S. Cachexia, muscle wasting, and frailty in cardiovascular disease. *Eur J Heart Fail*. 2020;22:2314-2326.

7. Valentova M, Anker SD and von Haehling S. Cardiac Cachexia Revisited: The Role of Wasting in Heart Failure. *Heart Fail Clin*. 2020;16:61-69.

8. Giglio Canelhas de Abreu L, Proenca Vieira L, Teixeira Gomes T and Bacal F. Clinical and Nutritional Factors Associated With Early Mortality After Heart Transplantation. *Transplant Proc*. 2017;49:874-877.

9. Lietz K, John R, Burke EA, Ankersmit JH, McCue JD, Naka Y, Oz MC, Mancini DM and Edwards NM. Pretransplant cachexia and morbid obesity are predictors of increased mortality after heart transplantation. *Transplantation*. 2001;72:277-83.

10. Grady KL, White-Williams C, Naftel D, Costanzo MR, Pitts D, Rayburn B, VanBakel A, Jaski B, Bourge R and Kirklin J. Are preoperative obesity and cachexia risk factors for post heart transplant morbidity and mortality: a multi-institutional study of preoperative weight-height indices. Cardiac Transplant Research Database (CTRD) Group. *J Heart Lung Transplant*. 1999;18:750-63.

11. Anker SD, Ponikowski P, Varney S, Chua TP, Clark AL, Webb-Peploe KM, Harrington D, Kox WJ, Poole-Wilson PA and Coats AJ. Wasting as independent risk factor for mortality in chronic heart failure. *Lancet*. 1997;349:1050-3.
12. Johnen H, Lin S, Kuffner T, Brown DA, Tsai VW, Bauskin AR, Wu L, Pankhurst G, Jiang L, Junankar S, Hunter M, Fairlie WD, Lee NJ, Enriquez RF, Baldock PA, Corey E, Apple FS, Murakami MM, Lin EJ, Wang C, During MJ, Sainsbury A, Herzog H and Breit SN. Tumor-induced anorexia and weight loss are mediated by the TGF-beta superfamily cytokine MIC-1. *Nat Med*. 2007;13:1333-40.
13. Macia L, Tsai VW, Nguyen AD, Johnen H, Kuffner T, Shi YC, Lin S, Herzog H, Brown DA, Breit SN and Sainsbury A. Macrophage inhibitory cytokine 1 (MIC-1/GDF15) decreases food intake, body weight and improves glucose tolerance in mice on normal & obesogenic diets. *PLoS One*. 2012;7:e34868.
14. Tsai VW, Macia L, Johnen H, Kuffner T, Manadhar R, Jorgensen SB, Lee-Ng KK, Zhang HP, Wu L, Marquis CP, Jiang L, Husaini Y, Lin S, Herzog H, Brown DA, Sainsbury A and Breit SN. TGF-b superfamily cytokine MIC-1/GDF15 is a physiological appetite and body weight regulator. *PLoS One*. 2013;8:e55174.
15. Patel S, Alvarez-Guaita A, Melvin A, Rimmington D, Dattilo A, Miedzybrodzka EL, Cimino I, Maurin AC, Roberts GP, Meek CL, Virtue S, Sparks LM, Parsons SA, Redman LM, Bray GA, Liou AP, Woods RM, Parry SA, Jeppesen PB, Kolnes AJ, Harding HP, Ron D, Vidal-Puig A, Reimann F, Gribble FM, Hulston CJ, Farooqi IS, Fafournoux P, Smith SR, Jensen J, Breen D, Wu Z, Zhang BB, Coll AP, Savage DB and O'Rahilly S. GDF15 Provides an Endocrine Signal of Nutritional Stress in Mice and Humans. *Cell Metab*. 2019;29:707-718 e8.

16. Borner T, Shaulson ED, Ghidewon MY, Barnett AB, Horn CC, Doyle RP, Grill HJ, Hayes MR and De Jonghe BC. GDF15 Induces Anorexia through Nausea and Emesis. *Cell Metab.* 2020;31:351-362 e5.
17. Emmerson PJ, Wang F, Du Y, Liu Q, Pickard RT, Gonciarz MD, Coskun T, Hamang MJ, Sindelar DK, Ballman KK, Foltz LA, Muppidi A, Alsina-Fernandez J, Barnard GC, Tang JX, Liu X, Mao X, Siegel R, Sloan JH, Mitchell PJ, Zhang BB, Gimeno RE, Shan B and Wu X. The metabolic effects of GDF15 are mediated by the orphan receptor GFRAL. *Nat Med.* 2017;23:1215-1219.
18. Hsu JY, Crawley S, Chen M, Ayupova DA, Lindhout DA, Higbee J, Kutach A, Joo W, Gao Z, Fu D, To C, Mondal K, Li B, Kekatpure A, Wang M, Laird T, Horner G, Chan J, McEntee M, Lopez M, Lakshminarasimhan D, White A, Wang SP, Yao J, Yie J, Matern H, Solloway M, Haldankar R, Parsons T, Tang J, Shen WD, Alice Chen Y, Tian H and Allan BB. Non-homeostatic body weight regulation through a brainstem-restricted receptor for GDF15. *Nature.* 2017;550:255-259.
19. Mullican SE, Lin-Schmidt X, Chin CN, Chavez JA, Furman JL, Armstrong AA, Beck SC, South VJ, Dinh TQ, Cash-Mason TD, Cavanaugh CR, Nelson S, Huang C, Hunter MJ and Rangwala SM. GFRAL is the receptor for GDF15 and the ligand promotes weight loss in mice and nonhuman primates. *Nat Med.* 2017;23:1150-1157.
20. Yang L, Chang CC, Sun Z, Madsen D, Zhu H, Padkjaer SB, Wu X, Huang T, Hultman K, Paulsen SJ, Wang J, Bugge A, Frantzen JB, Norgaard P, Jeppesen JF, Yang Z, Secher A, Chen H, Li X, John LM, Shan B, He Z, Gao X, Su J, Hansen KT, Yang W and Jorgensen SB. GFRAL is the receptor for GDF15 and is required for the anti-obesity effects of the ligand. *Nat Med.* 2017;23:1158-1166.

21. Wollert KC, Kempf T, Peter T, Olofsson S, James S, Johnston N, Lindahl B, Horn-Wichmann R, Brabant G, Simoons ML, Armstrong PW, Califf RM, Drexler H and Wallentin L. Prognostic value of growth-differentiation factor-15 in patients with non-ST-elevation acute coronary syndrome. *Circulation*. 2007;115:962-71.
22. Brown DA, Breit SN, Buring J, Fairlie WD, Bauskin AR, Liu T and Ridker PM. Concentration in plasma of macrophage inhibitory cytokine-1 and risk of cardiovascular events in women: a nested case-control study. *Lancet*. 2002;359:2159-63.
23. Wiklund FE, Bennet AM, Magnusson PK, Eriksson UK, Lindmark F, Wu L, Yaghoutifam N, Marquis CP, Stattin P, Pedersen NL, Adami HO, Gronberg H, Breit SN and Brown DA. Macrophage inhibitory cytokine-1 (MIC-1/GDF15): a new marker of all-cause mortality. *Aging Cell*. 2010;9:1057-64.
24. Rohatgi A, Patel P, Das SR, Ayers CR, Khera A, Martinez-Rumayor A, Berry JD, McGuire DK and de Lemos JA. Association of growth differentiation factor-15 with coronary atherosclerosis and mortality in a young, multiethnic population: observations from the Dallas Heart Study. *Clin Chem*. 2012;58:172-82.
25. Wang TJ, Wollert KC, Larson MG, Coglianese E, McCabe EL, Cheng S, Ho JE, Fradley MG, Ghorbani A, Xanthakis V, Kempf T, Benjamin EJ, Levy D, Vasani RS and Januzzi JL. Prognostic utility of novel biomarkers of cardiovascular stress: the Framingham Heart Study. *Circulation*. 2012;126:1596-604.
26. Ho JE, Hwang SJ, Wollert KC, Larson MG, Cheng S, Kempf T, Vasani RS, Januzzi JL, Wang TJ and Fox CS. Biomarkers of cardiovascular stress and incident chronic kidney disease. *Clin Chem*. 2013;59:1613-20.

27. Kempf T, Sinning JM, Quint A, Bickel C, Sinning C, Wild PS, Schnabel R, Lubos E, Rupprecht HJ, Munzel T, Drexler H, Blankenberg S and Wollert KC. Growth-differentiation factor-15 for risk stratification in patients with stable and unstable coronary heart disease: results from the AtheroGene study. *Circ Cardiovasc Genet.* 2009;2:286-92.
28. Schopfer DW, Ku IA, Regan M and Whooley MA. Growth differentiation factor 15 and cardiovascular events in patients with stable ischemic heart disease (The Heart and Soul Study). *Am Heart J.* 2014;167:186-192 e1.
29. Dallmeier D, Brenner H, Mons U, Rottbauer W, Koenig W and Rothenbacher D. Growth Differentiation Factor 15, Its 12-Month Relative Change, and Risk of Cardiovascular Events and Total Mortality in Patients with Stable Coronary Heart Disease: 10-Year Follow-up of the KAROLA Study. *Clin Chem.* 2016;62:982-92.
30. Farhan S, Freynhofer MK, Brozovic I, Bruno V, Vogel B, Tentzeris I, Baumgartner-Parzer S, Huber K and Kautzky-Willer A. Determinants of growth differentiation factor 15 in patients with stable and acute coronary artery disease. A prospective observational study. *Cardiovasc Diabetol.* 2016;15:60.
31. Hagstrom E, Held C, Stewart RA, Aylward PE, Budaj A, Cannon CP, Koenig W, Krug-Gourley S, Mohler ER, 3rd, Steg PG, Tarka E, Ostlund O, White HD, Siegbahn A, Wallentin L and Investigators S. Growth Differentiation Factor 15 Predicts All-Cause Morbidity and Mortality in Stable Coronary Heart Disease. *Clin Chem.* 2017;63:325-333.
32. Kempf T, Bjorklund E, Olofsson S, Lindahl B, Allhoff T, Peter T, Tongers J, Wollert KC and Wallentin L. Growth-differentiation factor-15 improves risk stratification in ST-segment elevation myocardial infarction. *Eur Heart J.* 2007;28:2858-65.

33. Khan SQ, Ng K, Dhillon O, Kelly D, Quinn P, Squire IB, Davies JE and Ng LL. Growth differentiation factor-15 as a prognostic marker in patients with acute myocardial infarction. *Eur Heart J*. 2009;30:1057-65.
34. Bonaca MP, Morrow DA, Braunwald E, Cannon CP, Jiang S, Breher S, Sabatine MS, Kempf T, Wallentin L and Wollert KC. Growth differentiation factor-15 and risk of recurrent events in patients stabilized after acute coronary syndrome: observations from PROVE IT-TIMI 22. *Arterioscler Thromb Vasc Biol*. 2011;31:203-10.
35. Fuernau G, Poenisch C, Eitel I, de Waha S, Desch S, Schuler G, Adams V, Werdan K, Zeymer U and Thiele H. Growth-differentiation factor 15 and osteoprotegerin in acute myocardial infarction complicated by cardiogenic shock: a biomarker substudy of the IABP-SHOCK II-trial. *Eur J Heart Fail*. 2014;16:880-7.
36. Hagstrom E, James SK, Bertilsson M, Becker RC, Himmelmann A, Husted S, Katus HA, Steg PG, Storey RF, Siegbahn A, Wallentin L and Investigators P. Growth differentiation factor-15 level predicts major bleeding and cardiovascular events in patients with acute coronary syndromes: results from the PLATO study. *Eur Heart J*. 2016;37:1325-33.
37. Baggen VJ, van den Bosch AE, Eindhoven JA, Schut AW, Cuypers JA, Witsenburg M, de Waart M, van Schaik RH, Zijlstra F, Boersma E and Roos-Hesselink JW. Prognostic Value of N-Terminal Pro-B-Type Natriuretic Peptide, Troponin-T, and Growth-Differentiation Factor 15 in Adult Congenital Heart Disease. *Circulation*. 2017;135:264-279.
38. Meyer SL, Wolff D, Ridderbos FS, Eshuis G, Hillege H, Willems TP, Ebels T, van Melle JP and Berger RMF. GDF-15 (Growth Differentiation Factor 15) Is Associated With Hospitalization and Mortality in Patients With a Fontan Circulation. *J Am Heart Assoc*. 2020;9:e015521.

39. Wallentin L, Hijazi Z, Andersson U, Alexander JH, De Caterina R, Hanna M, Horowitz JD, Hylek EM, Lopes RD, Asberg S, Granger CB, Siegbahn A and Investigators A. Growth differentiation factor 15, a marker of oxidative stress and inflammation, for risk assessment in patients with atrial fibrillation: insights from the Apixaban for Reduction in Stroke and Other Thromboembolic Events in Atrial Fibrillation (ARISTOTLE) trial. *Circulation*. 2014;130:1847-58.
40. Hijazi Z, Oldgren J, Andersson U, Connolly SJ, Eikelboom JW, Ezekowitz MD, Reilly PA, Yusuf S, Siegbahn A and Wallentin L. Growth-differentiation factor 15 and risk of major bleeding in atrial fibrillation: Insights from the Randomized Evaluation of Long-Term Anticoagulation Therapy (RE-LY) trial. *Am Heart J*. 2017;190:94-103.
41. Kempf T, von Haehling S, Peter T, Allhoff T, Cicoira M, Doehner W, Ponikowski P, Filippatos GS, Rozenlyt P, Drexler H, Anker SD and Wollert KC. Prognostic utility of growth differentiation factor-15 in patients with chronic heart failure. *J Am Coll Cardiol*. 2007;50:1054-60.
42. Foley PW, Stegemann B, Ng K, Ramachandran S, Proudler A, Frenneaux MP, Ng LL and Leyva F. Growth differentiation factor-15 predicts mortality and morbidity after cardiac resynchronization therapy. *Eur Heart J*. 2009;30:2749-57.
43. Anand IS, Kempf T, Rector TS, Tapken H, Allhoff T, Jantzen F, Kuskowski M, Cohn JN, Drexler H and Wollert KC. Serial measurement of growth-differentiation factor-15 in heart failure: relation to disease severity and prognosis in the Valsartan Heart Failure Trial. *Circulation*. 2010;122:1387-95.
44. Sharma A, Stevens SR, Lucas J, Fiuzat M, Adams KF, Whellan DJ, Donahue MP, Kitzman DW, Pina IL, Zannad F, Kraus WE, O'Connor CM and Felker GM. Utility of Growth

Differentiation Factor-15, A Marker of Oxidative Stress and Inflammation, in Chronic Heart Failure: Insights From the HF-ACTION Study. *JACC Heart Fail.* 2017;5:724-734.

45. Bouabdallaoui N, Claggett B, Zile MR, McMurray JJV, O'Meara E, Packer M, Prescott MF, Swedberg K, Solomon SD, Rouleau JL, Investigators P-H and Committees. Growth differentiation factor-15 is not modified by sacubitril/valsartan and is an independent marker of risk in patients with heart failure and reduced ejection fraction: the PARADIGM-HF trial. *Eur J Heart Fail.* 2018;20:1701-1709.

46. Xu J, Kimball TR, Lorenz JN, Brown DA, Bauskin AR, Klevitsky R, Hewett TE, Breit SN and Molkentin JD. GDF15/MIC-1 functions as a protective and antihypertrophic factor released from the myocardium in association with SMAD protein activation. *Circ Res.* 2006;98:342-50.

47. Kempf T, Eden M, Strelau J, Naguib M, Willenbockel C, Tongers J, Heineke J, Kotlarz D, Xu J, Molkentin JD, Niessen HW, Drexler H and Wollert KC. The transforming growth factor-beta superfamily member growth-differentiation factor-15 protects the heart from ischemia/reperfusion injury. *Circ Res.* 2006;98:351-60.

48. Kempf T, Zarbock A, Widera C, Butz S, Stadtmann A, Rossaint J, Bolomini-Vittori M, Korf-Klingebiel M, Napp LC, Hansen B, Kanwischer A, Bavendiek U, Beutel G, Hapke M, Sauer MG, Laudanna C, Hogg N, Vestweber D and Wollert KC. GDF-15 is an inhibitor of leukocyte integrin activation required for survival after myocardial infarction in mice. *Nat Med.* 2011;17:581-8.

49. Schmitt JP, Kamisago M, Asahi M, Li GH, Ahmad F, Mende U, Kranias EG, MacLennan DH, Seidman JG and Seidman CE. Dilated cardiomyopathy and heart failure caused by a mutation in phospholamban. *Science.* 2003;299:1410-3.

50. Truszkowska GT, Bilinska ZT, Kosinska J, Sleszycka J, Rydzanicz M, Sobieszczanska-Malek M, Franaszczyk M, Bilinska M, Stawinski P, Michalak E, Malek LA, Chmielewski P, Foss-Nieradko B, Machnicki MM, Stoklosa T, Poninska J, Szumowski L, Grzybowski J, Piwonski J, Drygas W, Zielinski T and Ploski R. A study in Polish patients with cardiomyopathy emphasizes pathogenicity of phospholamban (PLN) mutations at amino acid position 9 and low penetrance of heterozygous null PLN mutations. *BMC Med Genet.* 2015;16:21.
51. Fish M, Shaboodien G, Kraus S, Sliwa K, Seidman CE, Burke MA, Crotti L, Schwartz PJ and Mayosi BM. Mutation analysis of the phospholamban gene in 315 South Africans with dilated, hypertrophic, peripartum and arrhythmogenic right ventricular cardiomyopathies. *Sci Rep.* 2016;6:22235.
52. Burke MA, Chang S, Wakimoto H, Gorham JM, Conner DA, Christodoulou DC, Parfenov MG, DePalma SR, Eminaga S, Konno T, Seidman JG and Seidman CE. Molecular profiling of dilated cardiomyopathy that progresses to heart failure. *JCI Insight.* 2016;1.
53. Love MI, Huber W and Anders S. Moderated estimation of fold change and dispersion for RNA-seq data with DESeq2. *Genome Biol.* 2014;15:550.
54. Goetze JP, Bruneau BG, Ramos HR, Ogawa T, de Bold MK and de Bold AJ. Cardiac natriuretic peptides. *Nat Rev Cardiol.* 2020;17:698-717.